



TECHNISCHE UNIVERSITÄT MÜNCHEN

TUM

School of Medicine and Health

Anatomical reasons for technical failure of dual-filter cerebral embolic protection application in transcatheter aortic valve replacement: a CT-based analysis

Caterina Campanella

Vollständiger Abdruck der von der TUM School of Medicine and Health der Technischen Universität München zur Erlangung einer Doktorin der Medizin genehmigten Dissertation.

Vorsitz: apl. Prof. Dr. Ute Reuning

Prüfende der Dissertation:

1. Priv.-Doz. Dr. Keti Vitanova
2. Priv.-Doz. Dr. Teresa Trenkwalder

Die Dissertation wurde am 08.03.2023 bei der Technischen Universität München eingereicht und durch die Fakultät für Medizin am 30.09.2023 angenommen.

The results presented in this dissertation were based on the same dataset and working group as the paper of Voss et al published in the Journal of Cardiac surgery in 2021, leading to similarities in data presentation.

Voss S, Campanella C, Burri M, Trenkwalder T, Sideris K, Erlebach M, Ruge H, Krane M, Vitanova K, Lange R. Anatomical reasons for failure of dual-filter cerebral embolic protection application in TAVR: A CT-based analysis. *J Card Surg.* 2021 Dec;36(12):4537-4545. doi: 10.1111/jocs.16025. Epub 2021 Sep 27. PMID: 34580919.

Table of contents

Table of contents	3
Abbreviations	4
1 Introduction	5
1.1 Research endpoints.....	13
2 Material and methods	14
2.1 Sentinel Cerebral Protection System.....	14
2.1.1. Device specification and application.....	14
2.1.2. Indications and contraindications	16
2.2 Patients.....	18
2.3. 3- dimensional multislice computed tomography analysis	20
2.3.1. Aortic arch characteristics.....	21
2.3.1.1. Aortic arch anatomy.....	21
2.3.1.2. Aortic arch configuration.....	22
2.3.2. Take off angles	23
2.3.3 Vascular tortuosity	25
2.4 Intraobserver and interobserver correlation coefficient.....	27
2.5 Clinical data	27
2.6 Statistical analysis	28
3 Results	29
3.1 Patients characteristics.....	29
3.1.1 Procedural characteristics.....	29
3.2 Failure of Sentinel-CPS application	30
3.3 MSCT measurements	33
3.4 Intraclass Correlation Coefficient	36
4 Discussion	38
4.5 Limitations	43
5 Summary and Conclusion	44
6.List of figures	46
7.List of tables	48
8. References	49
9.Acknowledgments	58
10. Dissertation based paper	59

Abbreviations

AA/BA Angle Aortic arch/brachiocephalic artery angle

AA/CCA Angle Aortic arch/common carotid artery angle

AS Aortic stenosis

SAVR Surgical aortic valve replacement

BA/CCA Angle Brachiocephalic/common carotid artery angle

CAS Carotid artery stenting

CEPD cerebral embolic protection device

DW-MRI Diffusion Weight Magnetic resonance imaging

EACTS European Association for Cardio-Thoracic Surgery

EF Ejection fraction

GFR Glomerular Filtration Rate

ICC Intraclass correlation coefficient

LV Left ventricle

MRI Magnetic resonance imaging

MSCT Multislice computed tomography

ROC Receiver operating curve

RCT Randomized clinical trials

Sentinel-CPS Sentinel™ Cerebral Protection System

TAVR Transcatheter aortic valve replacement

TI Tortuosity Index

VARC Valve academy research consortium

1. Introduction

Calcific aortic valve stenosis is the most common valvular heart disease in the Western world and is increasing in prevalence due to the aging population [52]. Currently, the incidence is ranging between 2-7% in people over the age of 65 years [53,54] and up to 10% for people over the age of 80 years [55]. Once symptoms develop, it is associated with a dismal prognosis if patients remain untreated [56].

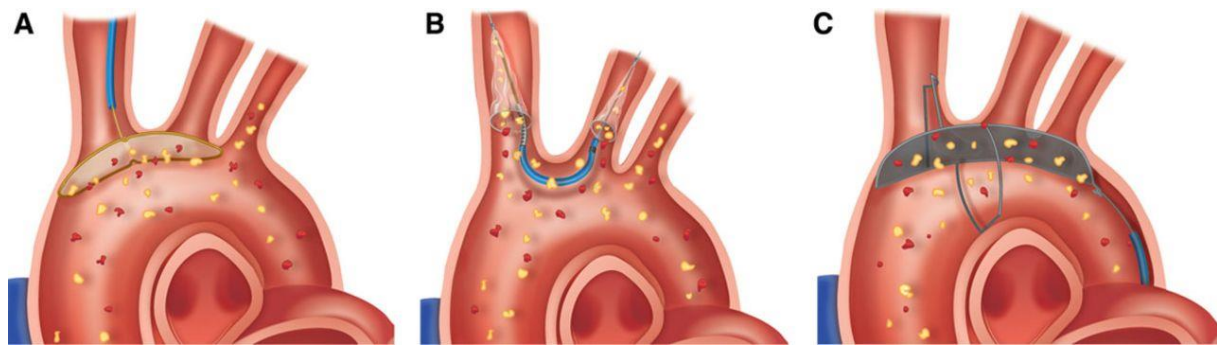
Surgical aortic valve replacement (SAVR) has become the gold standard for the treatment of severe calcific aortic stenosis [53]. However, there is a growing number of patients deemed unsuitable for a conventional surgical procedure due to significant comorbidities [6, 7]. The introduction of a minimally invasive transcatheter-based method [transcatheter aortic valve replacement (TAVR)] in 2002 has led to a paradigm shift in the treatment of patients at prohibitive risk for surgery [56]. As opposed to SAVR, TAVR is performed endovascularly under fluoroscopic control, without the need for thoracotomy and cardiopulmonary bypass [57.] The femoral approach (transfemoral) constitutes thereby the first line-TAVR access. After angiographic-guided puncture of the femoral artery, the TAVR prosthesis is introduced using special catheter delivery systems and is navigated retrogradely through the vasculature, across the aorta to the aortic valve root. The transcatheter heart valves (THVs) are comprised of a foldable bioprosthetic valve sewed into a balloon-expandable or self-expanding stent. THVs are used to be deployed under rapid pacing, once the valve is positioned under fluoroscopic guidance in a perpendicular projection to the aortic valve annulus. Rapid pacing is helpful to control blood pressure below 40 mmHg in order to avoid valve migration during deployment [58].

Although TAVR has emerged as an important treatment option in patients with aortic stenosis [9,10,44], periprocedural complications still occur. Cerebrovascular events are still among the most feared complications and are known to significantly affect survival and quality of life [11,12]. Cerebral embolization represents the presumed etiology of the majority of intraprocedural strokes [20]. During the procedure, corpuscular components such as calcified or atheromatous plaques can be dislodged and embolize into the brain-supplying vessels, ultimately causing ischemic stroke. Transcranial doppler monitoring in TAVR identified increased cerebral embolic load during retrograde passage of the aortic arch with catheters, as well as during positioning and deployment of the new prosthesis [59].

According to the latest updated Valve Academic Research Consortium (VARC-III) endpoint definitions [18], symptomatic stroke (overt stroke) is defined as an acute onset of focal neurological signs or symptoms with neuroimaging evidence of CNS infarction in the corresponding brain territory [18]. The incidence of symptomatic stroke associated with TAVR differs across various studies. In 2019 a large register study from the Society of Thoracic Surgeons/American College of Cardiology transcatheter valve Therapy (STS/TVT) analyzed over 7000 patients, reporting a procedural symptomatic stroke incidence of 2.3% [60,2,3]. This is in line with recent data of an all-comers analysis of the German heart center Munich, which observed an incidence of symptomatic stroke of 3.5% over the last decade. In this study the majority of strokes were territorial ischemic lesions (84.4%), with a left-sided hemisphere predilection of 45.6% [61].

Despite a relatively low incidence of clinically overt strokes, diffusion-weighted magnetic resonance imaging (DW-MRI) detected clinically asymptomatic infarctions (covert) in up to 84.0% of TAVR patients [62]. Asymptomatic or so called “covert” strokes are classified as new ischemic infarctions confirmed by neuroradiological imaging, without a corresponding insult syndrome (VARC III). Different from the stroke pattern in symptomatic patients, asymptomatic stroke patients usually show multiple, small, as well as bilaterally localized ischemic lesions in brain imaging [9]. However, asymptomatic embolic microlesions are thought to be associated with reduced cognitive function and long-term neurological impairment [62,63,56]. Thus, prevention of ischemic brain injury during TAVR procedure is imperative.

Over the years, adjuvant mechanical strategies have been developed in order to prevent periprocedural ischemic stroke [31, 32]. Dedicated filter-based and deflecting cerebral embolic protection devices (CEPD) are designed to reduce the cerebral burden of embolic debris by either capturing or deflecting embolized material travelling to the brain [13, 64] (Figure A). While filter-based devices have the advantage to trap and capture the embolized material (Figure 1B), deflector-devices redirect them towards the descending part of the aorta, carrying a risk of peripheral embolism (Figure 1A, 1C). CEPDs are usually positioned before THV implantation and retrieved at the end of the procedure.



[68] Figure 1, Fanning JP, et al. Characterization of neurological injury in transcatheter aortic valve implantation: how clear is the picture?

Figure 1.A: Embrella Embolic Deflector device (EED) (Edwards Lifesciences; Irvine, California, United States)

Figure 1.B: The Claret embolic protection device (CD) (Claret Medical, Inc.; Santa Rosa, California, United States)

Figure 1.C: The TriGuard (TG) CEPD (Keystone Heart Ltd., Herzliya, Israel)

Several new CEPD`s are under development or at the first-in-man study stage and include potentially promising devices designed to provide full body circumferential aortic protection. The earliest dedicated devices for TAVI were the deflector Embrella (Edwards Lifesciences, Irvine, CA, USA) (Figure 1.A), followed by another deflector type system, the TriGuard™ Embolic Deflection Device (Keystone Heart, Herzliya, Israel) (Figure 1.C) and the filter based Sentinel™ Cerebral Embolic Protection System (Boston Scientific, Corp., USA) (Fgiure 1.B). In recent years, all three devices have received CE approval.

Feasibility and safety of the Embrella device was evaluated in the prospective, non-randomized multicenter PROTAVI-C trial in 2014 (n=52) [67]. Introduced via the right radial artery, the Embrella system consists of two oval-shaped petals, placed at the outer curvature of the aortic arch, covering the ostia of the brachiocephalic trunk and the left common carotid artery. Although the device was successfully deployed in all patients (n=41), the EED (Embrella embolic device) did not prevent the occurrence of cerebral ischemic lesions [67]. New brain lesions by DW-MRI were found in 100% of patients. In addition, an increased total number of high-intensity transient signals (HITS) on transcranial doppler ultrasound was detected in the EED group, suggesting

that the Embrella device itself could be a potential source of embolic debris (632 [interquartile range: 347 to 893] HITS of EED group vs. 279 of the control group [interquartile range: 0 to 505] HITS, $p < 0.001$). Nowadays the EED is no longer commercially available [67].

Similar to the Embrella System, the TriGuard 3™ CEPD is a deflector type system, which provides full cerebral protection by covering all 3 branches of the aortic arch [41]. It consists of a single-wire nitinol frame and a filter with a semi-permeable mesh that deflects particles larger than 140µm.

A multicenter safety and performance evaluation of the first generation TriGuard™ Embolic Deflection Device (CEPD) (DEFLECT I) enrolled 37 consecutive patients, who underwent TAVR with TriGuard CEPD application. Device implantation was successful in 80% of the patients [69] and performance evaluation of the first-generation TriGuard device has led to Conformite´ Europeenne marking in October 2015. In the following years a new generation of the TriGuard EDD was developed and its superiority to the older device analyzed in the DEFLECT III study [65]. In comparison, the new generation EDD achieved a better vessel coverage in 89% of the patients vs a coverage of 80% with the previous generation [69]. Moreover, an intention to treat analysis demonstrated that the usage of Triguard CEPD was associated with greater freedom from new ischemic brain lesions (26.9% of TriGuard group vs 11.5% control group) and fewer new neurological deficits detected by the NIHSS (3.1% vs. 15.4%) [65] but without reaching statistical significance.

Consequently the DEFLECT III trial was able to show the safety of the early-generation TriGuard HDH CEPD but was not powered to demonstrated its efficacy [65].

Further on, the next device generation, the TriGUARD 3 (TG3), was designed to provide greater ease of use and stability with a larger filtration surface that self-

stabilizes without cerebral artery engagement. Its safety and feasibility were analyzed by the REFLECT II trial [70], in which 225 patients were randomized 2:1 (TG3 vs. no TG3) in a prospective, multicenter analysis. Nevertheless, also in this study despite the promising results and the confirmed primary 30-day safety endpoints (VARC II), the new generation TG3 failed to meet its pre-specified primary superiority efficacy endpoint (mean scores [higher is better]: 8.58 TG3 vs. 8.08 control; $p = 0.857$)[70].

Nowadays, the most used cerebral embolic protection device is the dual-filter based Sentinel™ Cerebral Protection System (Sentinel-CPS) (Boston Scientific, Marlborough, MA, USA) and so far, the only neuroprotection device with an approval by the Food and Drug Administration. The system is inserted through the right radial or brachial artery and the filters are targeted to the brachiocephalic (proximal target vessel) and the left common carotid artery (distal target vessel) in order to capture and remove embolic debris while performing TAVR.

In the past, three randomized clinical trials (RCT) investigated the filter- based Sentinel CPS. New cerebral lesions on diffusion-weighted MRI (DW-MRI) were considered as a common surrogate parameter for the occurrence of periprocedural neurologic damage during TAVR in all 3 studies. In 2016, the randomized, single center CLEAN-TAVI trial (n=100) demonstrated a significant reduction in number and volume of new ischemic brain lesions within protected areas in the Sentinel group compared to the unprotected cohort using the second generation filter device [7]. The third generation system was investigated in a multicenter double blinded, randomized trial (MISTRAL-C), which analyzed 65 patients undergoing TAVR with and without Sentinel-CPS. DW-MRI examinations revealed a decrease of new ischemic infarctions and a smaller infarction volume in patients receiving protected TAVR, but without statistical significance [71]. Hereafter, the SENTINEL trial was initiated to assess the safety of

cerebral embolic protection during TAVR and the efficacy of filter coverage in reducing the effects of cerebral embolization in a larger multicenter RCT (n=363). This landmark trial confirmed reassuring evidence of the safety of Sentinel-CPS usage and demonstrated a high-frequency of embolic debris capture in 99% of patients [1]. However, the primary efficacy endpoint, defined as a reduction in median total lesion volume in brain areas protected by Sentinel CPS, could not be achieved [6]. Similar to CLEAN TAVI [7] and MISTRAL C [71], the SENTINEL study [1] also failed to demonstrate a reduction in clinically symptomatic stroke rates. However, all of these RCT's have not been designed for hard clinical endpoints to unequivocally show the impact of CEP on periprocedural stroke incidence.

Therefore, the PROTECTED TAVR [72] was designed to specifically evaluate the efficacy of the Sentinel CEPS device in reducing strokes among patients undergoing transfemoral TAVR. The PROTECTED TAVR trial is so far the biggest randomized trial assessing a cerebral embolic protection device, involving 3000 patients, who were randomized in 1:1 fashion to either the CEP (n = 1,501) group or control group (n = 1,499). This analysis was able to confirm a reduction in clinical symptomatic strokes within 72 hours after TAVR or before discharge, in patients receiving the CEP device (strokes occurred in 34 patients in the CEP group vs in 43 in the control cohort, p=0.30) and in the same group to show also a statistical relevant less incidence of disabling stroke [strokes [8 (0.5%) in the CEP group vs 20 (1.3%) in the control group, p < 0.05].

Currently the debate over a routine use of the dual filter Sentinel, together with its safety and feasibility features, is still on going. Parallel newer studies have been focusing on the identification of procedural preconditions, as well as for risk factors that could potentially prevent the device implantation [44,9].

A recent all-comers analysis by Voss and colleagues determined the percentage of patients potentially eligible for routine Sentinel-CPS implantation according to the official instructions for use. Clinical data and MSCT analysis in 317 consecutive patients evinced device compatibility in 61.5% (n=122/317). The most common reason for potential Sentinel-CPS treatment exclusion was an inappropriate diameter within the target landing zone of the left carotid artery (< 6.5 mm) (28%). As there is currently only one size of filter system available, only 2/3 of patients might be eligible for routine Sentinel-CPS usage. Even if the official criteria for Sentinel CPS implantation are met, a complex anatomy of the aortic arch and the supra-aortic vessels might challenge its application [7-9]. Especially vascular tortuosity of the supra-aortic vessels has been reported to cause failure of Sentinel CPS implantation due to technical difficulties to navigate the catheter. Besides the unfavorable anatomic conditions, repeated wire exchanges and special maneuvers might expose the patient to a higher risk of atheroembolism from the aortic arch and vessel injury [7,10,11]. Thus, it is important to identify patients that have an anatomical barrier before starting Sentinel-CPS implantation. To date, there is no objective evidence of vascular anatomy and potential cut-off values that might be associated with technical failure of Sentinel-CPS implantation.

1.2. Research endpoints

Considering the above established concepts and themes around stroke preventions in TAVR patients we sought to investigate the impact of anatomic features of the aortic arch and the supra-aortic arteries observed on pre-TAVR multislice computed tomography (MSCT) aortograms on technical device failure of Sentinel-CPS application in patients undergoing TAVR.

More specific, this research concentrated on addressing the following issues:

1. Incidence of Sentinel-CPS failure in patients undergoing TAVR.
2. Evaluation of anatomical characteristic of the aortic arch and the supraaortic arteries potentially associated with failure of Sentinel CPS application.
3. Calculation of potential cut-off values influencing the procedural success of Sentinel-CPS application.

2. Materials and Methods

2.1. Sentinel™ Cerebral Protection System

2.1.1. Device specification and application

The 3rd generation Sentinel-CPS (Boston Scientific, Marlborough, MA, USA) consists of a steerable catheter (100 cm) carrying two cone-shaped, radiopaque, nitinol-coated and biocompatible polyurethane filters equipped with 140- μ m pores [6,13]. The proximal filter has a maximum diameter of 15mm, whereas the distal one has a diameter of 10mm (Figure 1).

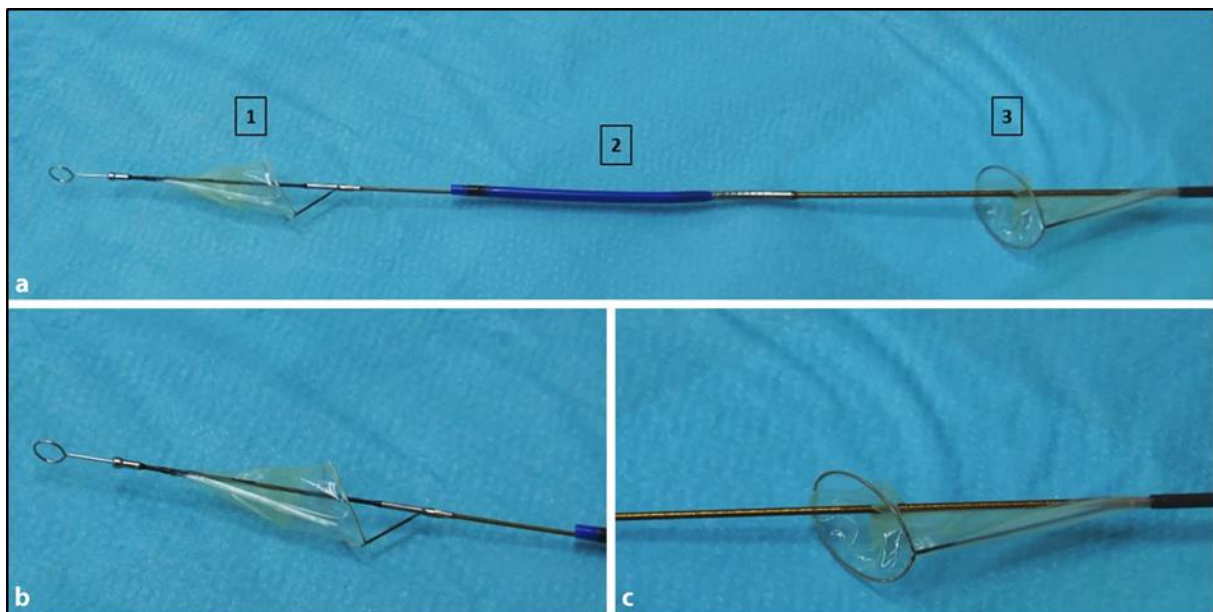


Figure 2, Sentinel™ Cerebral Protection System

(a) Distal filter (1), steerable catheter (100 cm) (2) and proximal filter (3). (b+c) two cone-shaped filter made of a radiopaque Nitinol coat biocompatible polyurethane (with 140- μ m pores) with a maximum diameter of 10mm distal (b) and 15mm proximal (c)⁴⁷

Sentinel-CPS implantation is performed angiographically with the use of contrast agent. Prior to device insertion an anticoagulation with heparin is needed to achieve a systemic Activated Clotting Time (ACT) of 250 seconds. For Sentinel-CPS application a 6-Fr- sheath is placed in the right radial or brachial artery. After flushing the catheter

and the filters, the device is introduced over a standard a 0.014” coronary guide wire [6,13,14]. The device catheter is then advanced into the aortic arch and the proximal filter is deployed in the brachiocephalic trunk. By using the integrated articulation sheath, the distal part of the catheter is flexed and placed into the ostium of the left common carotid artery [13, 14], where the second filter (distal) is deployed. The radiopaque markers on both filters allow their correct placement in the corresponding filter landing zones.

Filter landing zone of the distal and proximal filter is defined as the area of the brachiocephalic trunk and left common carotid artery from their origin at the aortic arch to the brachiocephalic bifurcation, and up to 40mm of length for the left common carotid artery, respectively.

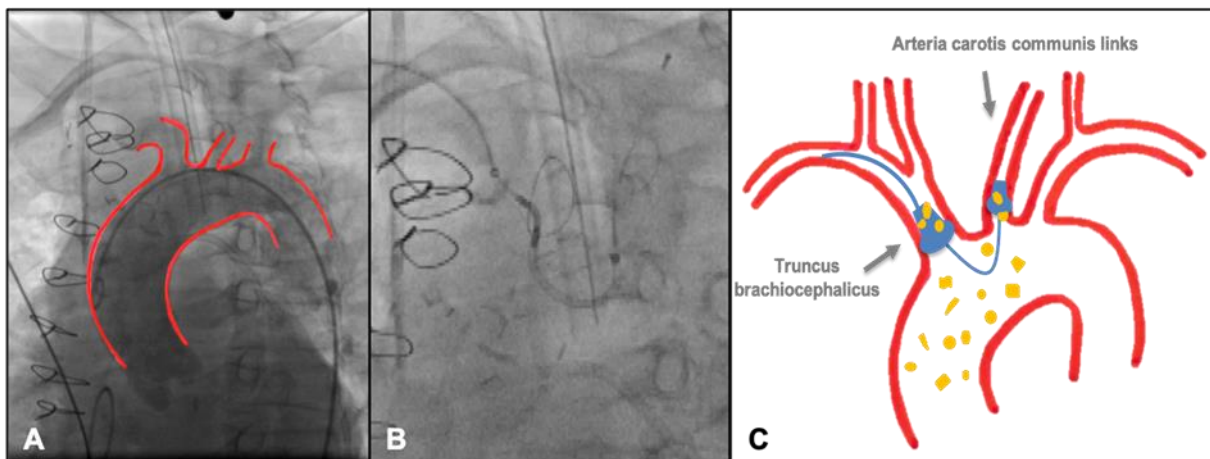


Figure 3: Filterlanding zone in the aimed vessel, Voss.S. (2022) Neuroprotektion bei Transkatheter-Aortenklappenimplantation (Habilitation, Technische Universität München)

(A) Aortic arch identification, (B) Deployment of both filters in the aimed vessels (C) graphic representation of filterdeployment

After finishing TAVR procedure, both filters can be retrieved and the whole device is extracted. The Sentinel CPS device received European CE mark in 2014 and is currently available in one universal size.

2.1.2. Indications and contraindications for Sentinel-CPS usage

Sentinel-CPS is indicated as an embolic protection device to capture and remove thrombotic debris while performing transcatheter aortic valve replacement procedures, unless contraindicated [1,5,12,41].

Pre-TAVR multislice computed tomography (CT) aortograms are used to determine patient eligibility for Sentinel CPS implantation. CT morphological preconditions for application of the dual-filter-based protection device according to the official instructions for use are [20]:

- absence of significant carotid or brachiocephalic artery stenosis (>70%)
- absence of severe calcifications of the target vessels
- freedom of dissections or aneurysmatic alterations at the origin of the brachiocephalic and/or left carotid artery
- absence of a true bovine arch (a common single brachiocephalic trunk that trifurcates into bilateral subclavian arteries and a single bicarotid trunk).
- absence of an aberrant right subclavian artery
- proximal filter landing zone <9mm and >15mm
- distal filter landing zone < 6,5mm and >10mm

In addition, presence of vascular alterations precluding the insertion of the CPS Sentinel device are considered clinical exclusion criteria [20]:

- history of previous artery repair in a vessel used for device implantation or filter deployment
- compromised blood flow to the right upper extremity
- arteriovenous fistulas
- arteries used for dialysis purpose
- hypersensitivity to nickel-titanium

2.2 Patients

This retrospective analysis was conducted at the Department of Cardiovascular Surgery at the German Heart Center Munich. We identified all patients, who underwent transfemoral TAVR with Sentinel-CPS usage between February 2016 and February 2020 from our institutional TAVR database.

To determine the impact of vascular anatomy on technical failure of Sentinel-CPS application, a systematic MSCT analysis of pre-TAVR aortograms was performed.

The study complied with the Declaration of Helsinki and was approved by the local ethics committee of the Technical University of Munich (approval reference number: 49/20 S-KH).

Sentinel-CPS application was performed in 92 patients [44]. All patients fulfilled the criteria for Sentinel-CPS implantation according to the instructions for use and had no contraindications. The dual-filter protection device was used in 14 patients with an increased risk for cerebral embolization due to:

- severely calcific aortic valves ($n = 6$)
- history of previous stroke ($n = 2$)
- thromboembolic deposits on the aortic valve ($n = 1$)
- significant bioprosthetic aortic valve degeneration ($n = 3$)
- porcelain aorta ($n = 2$).

Further Sentinel-CPS usage ($n = 78$) was practiced as part of our ongoing single-center, randomized PROTECT TAVI trial (clinicaltrials.gov NCT02895737 328), in which patients are randomly assigned to either undergo TAVR with a balloon-expandable or a self-expandable valve, with and without Sentinel-CPS.

The study population was further divided into two groups [44]:

1. Sentinel-CPS success group, in which the application of the Sentinel-CPS was achieved ($n = 83$)
2. Sentinel-CPS failure group, in which application of Sentinel-CPS was not successful. ($n = 9$)

2.3 Three-dimensional MSCT analysis

All MSCT data were evaluated using automated software for 3-dimensional CT reconstruction (3mensio structural heart version 10.2, Pie Medical Imaging, Maastrich, The Netherlands).

The subclavian route model was used to enable the visualization of the anatomical target vessels (subclavian artery, brachiocephalic trunk, left common carotid artery, aortic arch). By selecting the required vessel, the software automatically displayed a central line along the vascular lumen. Manual adjustment of the centerline was made to obtain the most accurate measurement [44] (Figure 4).

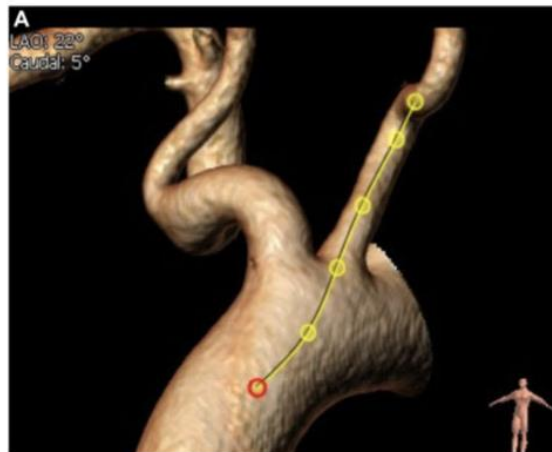


Figure 4 from S.Voss et al, interactive cardiovascular and thoracic surgery, multislice computed tomography measurements using the automated 3mensio software. (A) Centre line across the lumen of the distal target

2.3.1. Aortic arch characteristics

2.3.1.1. Aortic arch anatomy

Aortic arch anatomy was evaluated on a 3-D volume rendering view and classified as follows:

- Normal aortic arch: separated origins for the brachiocephalic, left common carotid, and left subclavian arteries (Figure 5A)
- Bovine arch Type I: common origin for the brachiocephalic and left common carotid artery (Figure 5B)
- Bovine arch Type II: common origin of the brachiocephalic and left common carotid artery, with the left common carotid artery bifurcating at an average distance of ≤ 1 cm from the origin (Figure 5C)



Figure 5, multislice computed tomography measurements using the automated 3mensio software: (A) normal aortic arch, (B) bovine arch Type I, (C) bovine arch type II.

2.3.1.2. Aortic arch configuration

Arch configuration according to Müller et al was assessed by drawing two horizontal lines identifying the highest point of the outer and inner curvature of the aortic arch [44,15] (Figure 6). To obtain the most accurate measurement, evaluation of arch configuration was performed in the sagittal plane as well as in the 3-dimensional volume rendering view

Aortic arch configuration was then classified as follow:

- Type 1 configuration: if all supra-aortic branches originate from the arch at the level of the upper horizontal line
- Type 2 configuration: if at least one of the supra-aortic branches originates between the two lines and
- Type 3 configuration: if at least one of the supra-aortic branches originates at the level or below the lower line [44,15] (Figure 6).

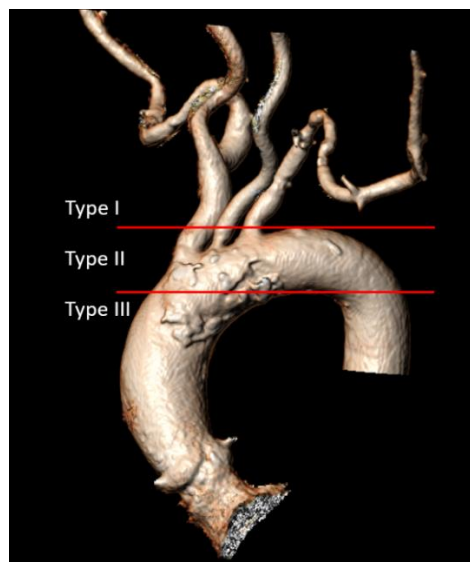


Figure 6 from S.Voss et al, interactive cardiovascular and thoracic surgery, multislice computed tomography measurements using the automated 3mensio software, Aortic arch type

2.3.2. Take-off angles of the supra-aortic arteries

Further analysis included the assessment of the following angles:

- AA/BA angle: angle between the aortic arch (AA) and the brachiocephalic artery (BA)
- AA/CCA angle: angle between the aortic arch (AA) and the left common carotid artery (CCA)
- BA/CCA angle: inner great vessel angle between the BA and the left CCA

For determination of the take-off angles (AA/BA angle; AA/CCA angle) a straight line was drawn connecting the external origin of the left subclavian and the brachiocephalic artery in the sagittal view. The accurate positioning of the reference points was verified in the axial and coronal planes [44]. Then a central line across the vessel lumen of the corresponding supra-aortic branch was generated to determine the distal vascular course. To measure the corresponding angle, one angle leg was placed distally following the previously marked central course of either the brachiocephalic or the left common carotid artery and one angle leg was positioned parallel to the previously drawn straight baseline [44,15] (Figure 7).

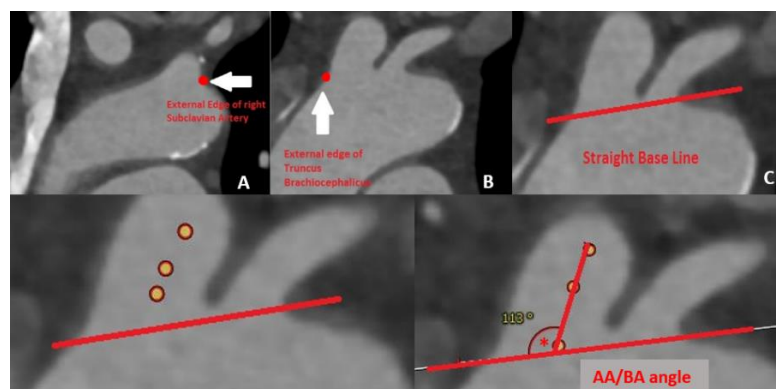


Figure 7, from S.Voss et al, interactive cardiovascular and thoracic surgery, multislice computed tomography measurements using the automated 3mensio software: Measurements of the take-off angles

The inner great vessel angle (BA/CCA angle, Figure 8) was calculated using the 3-mensio angle measurement tool. We measured the most pronounced 3-dimensional angle along the central course of the originating part of the brachiocephalic artery, the aortic arch and the originating part of the left common carotid artery [44].

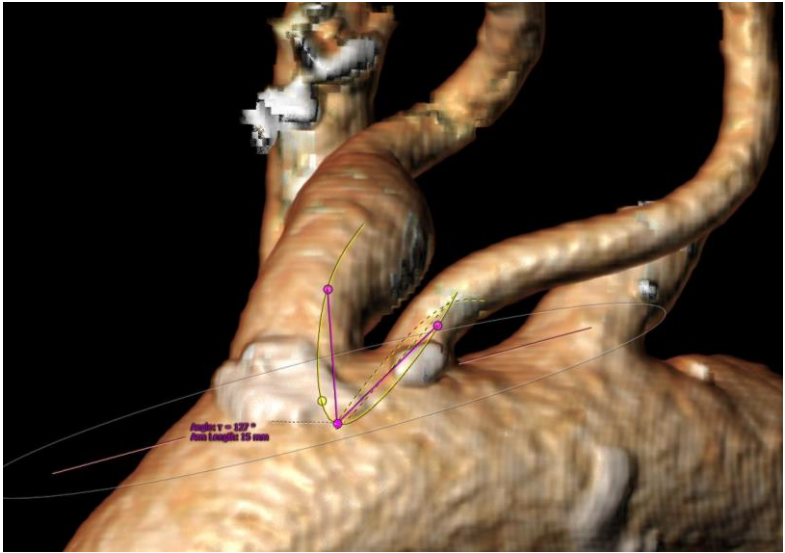


Figure 8, multislice computed tomography measurements using the automated 3mensio software: Inner great vessel angle (BA/CCA)

2.3.3. Vascular tortuosity

Vascular tortuosity was assessed in the area of the filter target vessels and the right subclavian artery. The 3-mensio tortuosity angle tool served to quantify the extent of 3-dimensional tortuosity in the vessels. The software used the previously defined central line with a given point and 2 evenly spaced points, creating 15mm arms in opposite directions of the former given point [44]. By scrolling the given point up and down across the central line, the maximal tortuosity angle of the according vasculature could be detected (Figure 9A).

According to the filter landing zones of the corresponding target vessel the left common carotid artery was evaluated from its origin from the aortic arch until 40mm upwards along the vessel course. The brachiocephalic artery was evaluated from its origin at the aortic arch until its bifurcation into right subclavian and right common carotid artery. The right subclavian artery was evaluated along its course originating from brachiocephalic artery until the level of the humeral head. Besides the maximal tortuosity angle, a tortuosity index (TI) was assessed [44]. Brachiocephalic and left common carotid artery TI was determined by calculating a distance factor: $[(\text{centre-line distance}) / (\text{straight-line distance}) - 1] \times 100$ [16] (Figure 9B). Right subclavian TI was defined as the sum of all tortuosity angles along its course ($\Sigma = \alpha_1 + \alpha_2 + \alpha_3 + \dots + \alpha_n$) [17] (Figure 9C).

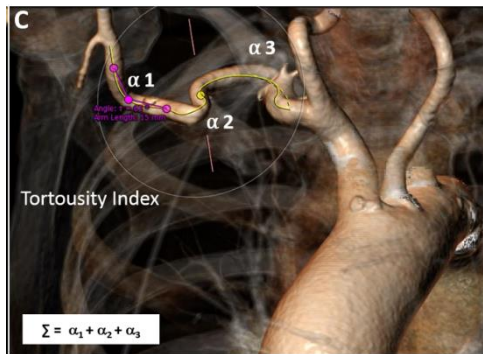
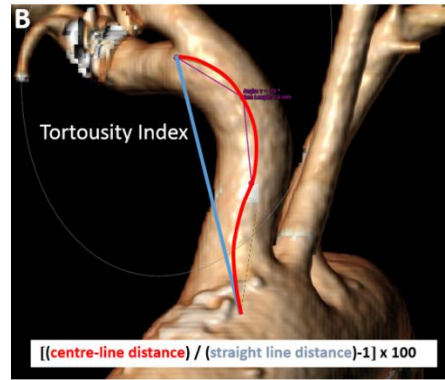
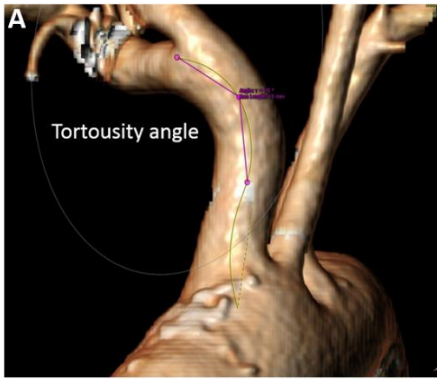


Figure 9, from S.Voss et al, interactive cardiovascular and thoracic surgery, multislice computed tomography measurements using the automated 3mensio software: (A) Tortuosity Angle, (B) Tortuosity Index of brachiocephalic trunk (C) Tortuosity Index of the right subclavian artery

2.4. Interobserver and intraobserver agreement

All measurements were done by two independent cardiac surgeons experienced in cardiovascular imaging. Inter- and intraobserver reliability for MSCT measurements was evaluated by calculating the inter- and intraclass correlation coefficient (ICC) as described by Koo TK et al [18]. Therefore, data from 15 randomly selected patients were remeasured by another observer and by the same observer at two different time points, respectively.

2.5 Clinical data analysis

Patient data were collected from the electronic medical record. Baseline factors analyzed were patient age, sex, weight, Logistic EuroSCORE, Society of Thoracic Surgeons Score, EuroSCORE II, glomerular filtration rate, history of stroke and peripheral arterial disease. Operative factors were the following: access routes for TAVR, type of transcatheter heart valve implanted, total fluoroscopy/procedure time, amount of contrasts used, dose area product ($\mu\text{g}/\text{cm}^2$) and reasons for failure of Sentinel-CPS application. Failure of Sentinel-CPS application was defined as the inability to insert the system and correctly deploy both filters in the proximal and distal target vessel[44].

2.6 Statistical analysis

Frequencies are listed as absolute numbers and percentages, continuous data are given as median and range. Normality of distributions for continuous variables was tested using the Shapiro-Wilks test, and data were analyzed appropriately using either the two-sided t-test or the Wilcoxon rank-sum test. We compared categorical variables using Fisher's exact test. ICC estimates and their 95% confident intervals (CI) were calculated based on the two-way random effects, absolute agreement, multiple raters / measurements ICC model (2,k) [18]. ICC values were classified as:

1. Values < below 0.5 as poor reliability
2. Values between 0.5 and 0.75 as moderate reliability
3. Values between 0.75 and 0.9 as good reliability
4. Values above 0.90 as excellent reliability.

Statistical analysis was performed by using IBM SPSS Statistics 25.0 software (IBM Corp, Armonk, NY). A P-value less than 0.05 was considered statistically significant

3. Results

3.1 Patient characteristics

A total of 97 patients underwent transfemoral TAVR with Sentinel-CPS usage at our institution between February 2016 and February 2020. 5 patients were excluded from the analysis due to insufficient quality of their MSCT datasets. The final study cohort included 92 patients divided into [44]:

1. Sentinel-CPS success group (n=83)
1. Sentinel-CPS failure group (n=9)

Mean age of the study cohort was 79.0 ± 7.0 years with a median logistic EuroSCORE and Society of Thoracic Surgeons Predicted Risk of Mortality Score of 2.7 [1.0–27.3] and 2.5 [0.8–12.4], respectively. Further baseline data are provided in Table 1 [44].

Table 1.

Patient characteristics	Sentinel-CPS success n=83	Sentinel-CPS failure n=9	P-value
Age, years (median, range)	79.0±7.0	82.0±6.0	0.266
Female, n (%)	40 (48.2)	7 (77.8)	0.159
Body mass index, kg/m ² (median, range)	26.1±4.3	29.3±7.8	0.266
Peripheral arterial disease, n (%)	13 (15.7)	0 (0.0)	0.349
History of stroke, n (%)	6 (7.2)	1 (11.1)	0.526
Society of Thoracic Surgeons Score (median, range)	2.5 [0.8-12.4]	2.3 [1.8-4.7]	0.655
Logistic EuroSCORE (median, range)	11.0 [1.7-46.0]	8.9 [4.3-25.1]	0.703
EuroSCORE II (median, range)	2.6 [1.0-27.3]	3.0 [1.5-5.7]	0.803

3.2. Procedural characteristics

Transcatheter heart valves implanted were the Edwards Sapien 3 (n=40), the Edwards Sapien Ultra (n=5), the Medtronic CoreValve™ (n=1) and the Medtronic CoreValve™ Evolut™ R (n=46). Total operation time did not differ significantly between the two groups. Fluoroscopy time, and amount of contrast dye are listed in detail in Table 2 [44] and did also not differ between TAVR patients with and without procedural success of Sentinel-CPS usage.

Table 2:

Procedural characteristics	Sentinel-CPS success n=83	Sentinel-CPS failure n=9	P-value
Self-expandable valve (CoreValve/Evolut R), n (%)	43 (51.8)	4 (44.5)	0.736
Balloon-expandable valve (Sapien 3/ Sapien Ultra), n (%)	40 (48.2)	5 (55.5)	
Total procedure time, min (median, range)	73 [46-248]	70 [53-84]	0.572
Total fluoroscopy time, min (median, range)	18 [9-54]	21 [15-276]	0.078
Amount of contrast agent, ml (median, range)	132 [75-165]	130 [105-160]	0.790
Dose area product, $\mu\text{gy}/\text{cm}^2$ (median, range)	3825 [687-16794]	3118 [1533-16695]	0.767

In 83 patients (90.2%), the Sentinel-CPS device was successfully delivered to the aortic arch and both filters were correctly positioned in the brachiocephalic and left carotid arteries [44]. Failure of Sentinel-CPS application occurred in 9.8% of patients (n=9). In 2 patients failure of Sentinel CPS insertion was due to significant kinking of

the right radial artery. Vascular tortuosity of the supra-aortic vessels made the deployment of both filters impossible in 6 patients. In one patient, positioning of the proximal filter was successful, whereas the deployment of the distal one failed due to carotid artery tortuosity. Retraction of the device was uneventful in all patients.

Detailed procedural and anatomic characteristics in patients with Sentinel-CPS failure (n=9) are summarized in Table 3[44].

Table 3: Intraoperative reasons for Sentinel-CPS failure

	Intraoperative reasons for Sentinel-CPS failure	Aortic arch anatomy	Brachiocephalic tortuosity > 59°	Subclavian TI > 191
<i>Patient 1</i>	Brachiocephalic tortuosity prevented correct deployment of both filters	Normal	Yes (80°)	No (191)
<i>Patient 2</i>	Excessive kinking of the right radial artery prevented advancement of the Sentinel-CPS to the filter target vessels	Normal	No (22°)	No (92)
<i>Patient 3</i>	Brachiocephalic tortuosity prevented correct deployment of both filters	Normal	Yes (78°)	No (107)
<i>Patient 4</i>	Excessive kinking of the right radial artery prevented advancement of the Sentinel-CPS to the filter target vessels	Normal	No (40°)	Yes (249)
<i>Patient 5</i>	Subclavian and brachiocephalic tortuosity prevented correct deployment of both filters	Normal	No (46°)	Yes (311)
<i>Patient 6</i>	Subclavian and brachiocephalic tortuosity prevented correct deployment of both filters	Bovine I	No (43°)	Yes (217)
<i>Patient 7</i>	Brachiocephalic tortuosity prevented correct deployment of both filters	Bovine I	Yes (69°)	No (193)
<i>Patient 8</i>	Brachiocephalic and carotid tortuosity prevented correct deployment of the distal filter*	Normal	Yes (75°)	Yes (232)
<i>Patient 9</i>	Brachiocephalic tortuosity prevented correct deployment of both filters	Normal	Yes (59°)	Yes (324)

3.3. MSCT measurements

The majority of patients had a normal aortic arch anatomy (79.4%, n=73), whereas 20.6% (n= 19) had a bovine arch variation, with n=17 showing a bovine type I and n= 2 a bovine type II anatomy.

Aortic arch configuration Type I was found in 15 patients (16.3%). Aortic arch configuration type II represents the major configuration (n=75, 81.5%) and aortic arch configuration type III was present in only 2 patients (2.2%). Distribution of type of anatomy and aortic arch configuration in the Sentinel CPS success and failure group is listed in Table 4.

MSCT measurement revealed no difference regarding the anatomy and configuration of the aortic arch in TAVR patients with Sentinel-CPS success (n=83) and device failure (n=9) (Table 4). Also, the supra-aortic take-off angles (AA/BA angle, AA/CCA angle) and the inner great vessel angle (BA/CCA angle) did not differ between the two groups (p=0.318, p=0.498, p=0.076). Evaluation of vascular tortuosity identified a significantly larger median brachiocephalic tortuosity angle (59° [22°-80°] vs. 39° [7°-104°], p=0.014) (Figure 4) and a significantly higher median brachiocephalic (27 [5-51] vs. 10 [0-102], p=0.033) and right subclavian TI (217 [92-324] vs. 150 [42-252], p=0.046) in patients with failure of Sentinel-CPS application compared to patients with successful deployment. Tortuosity measurements of the left common carotid artery were similar in both groups, showing no statistically significant difference (Table 3). Using the ROC analysis, a brachiocephalic angle > 59°, a brachiocephalic TI > 26 and a right subclavian TI > 191 were identified as predictors for technical device failure with a sensitivity and specificity of 71.4% and 91.5%, 71.4% and 90.3%, and 85.7% and 79.2%, respectively (Figure 9). The area under the curve (AUC) was 0.86 for the

brachiocephalic angle, 0.81 for the brachiocephalic, and 0.81 for the right subclavian TI.

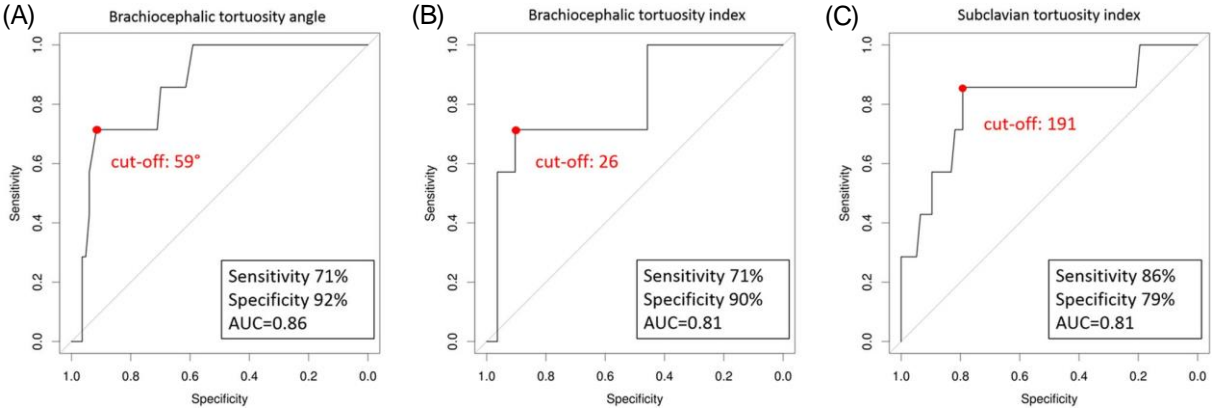


Figure 10 from S.Voss et al, interactive cardiovascular and thoracic surgery: Receiver operating characteristic curve (ROC) analysis for the brachiocephalic tortuosity angle (A), the brachiocephalic tortuosity index (B), and the subclavian tortuosity index (C). ROC analysis was only performed in patients with Sentinel™ Cerebral Protection System failure due to vascular tortuosity (n = 7)

Table 4: Aortic Arch Anatomy and aortic arch configuration [44].

Aortic Arch Anatomy	Sentinel-CPS success n=83	Sentinel-CPS failure n=9	P-value
Normal	66(79.5%)	7(77.8%)	1.000
Bovine type1	15(18.1%)	2(22.2%)	0.670
Bovine type 2	2(2.4%)	0(0.0%)	1.000
Aortic Arch Configuration	Sentinel-CPS success n=83	Sentinel-CPS failure n=9	P-value
Type 1	12(14.6%)	3(33.3%)	0.164
Type 2	69(83.1%)	6(66.7%)	0.361
Type 3	2(2.4%)	0(0.0%)	1.000

3.4. Inter- and intraobserver coefficient

The overall inter- and intraobserver reproducibility for all MSCT measurements was excellent with a mean ICC of 0.975 and 0.932, respectively. Estimated inter- and intraobserver agreement for each MSCT parameter including their 95% confident intervals is given in Table 5 and 6.

Table 5: Intraobserver agreement for 3-dimensional multislice computed tomography measurements [44].

Parameters	Intraclass Correlation Coefficient	95% Confidence Interval	
		Lower Bound	Upper Bound
Brachiocephalic tortuosity angle	0.986	0.758	0.997
Brachiocephalic tortuosity index	0.924	0.795	0.974
Left common carotid tortuosity angle	0.960	0.890	0.986
Left common carotid tortuosity index	0.743	0.387	0.906
Take-off angle BA/CCA	0.949	0.859	0.982
Take-off angle AA/BA	0.983	0.946	0.994
Take-off angle AA/CCA	0.950	0.855	0.983
Right subclavian tortuosity index	0.965	0.895	0.988

Table 6: Interobserver agreement for 3-dimensional multislice computed tomography measurements[44]

Parameters	Interclass Correlation Coefficient	95% Confidence Interval	
		Lower Bound	Upper Bound
Brachiocephalic tortuosity angle	0.990	0.970	0.997
Brachiocephalic tortuosity index	0.980	0.940	0.993
Left common carotid tortuosity angle	0.985	0.955	0.995
Left common carotid tortuosity index	0.952	0.855	0.984
Take-off angle BA/CCA	0.973	0.923	0.991
Take-off angle AA/BA	0.974	0.922	0.991
Take-off angle AA/CCA	0.970	0.909	0.990
Right subclavian tortuosity index	0.975	0.900	0.992

4.Discussion

Transcatheter aortic valve replacement is the golden standard for treating severe aortic stenosis in high risk patients and has been rapidly evolving and expanding towards intermediate and lower risk patient groups [53,56,6,7].

Interactions between the deployment of the new prosthesis and crush of the native valve behind the prosthesis frame and the aorta, might liberate small calcified fragments into the blood circulation, which cause the most featured TAVR complication, embolic stroke [73]. Neurovascular events after TAVR have been reported up to date with an incidence of 2,3% [60,2,3]. Even higher rates of embolization have been detected on DW-MRI studies, showing silent brain lesions in 84% of TAVR patients leading to long term neurological impairment and cognitive dysfunction [1,56,62,63].

As most cerebrovascular events occur perioperatively during TAVI implantation, it is imperative to protect the brain with cerebral embolic protection systems. In 2017, the U.S. Food and Drug Administration approved the dual-filter Sentinel-CPS. Since then, several studies have demonstrated that the Sentinel-CPS is safe [1, 5,7,67,72,] and effective in reducing cerebral injury [1,72], favouring routine use amongst all TAVR patients.

Moreover, the easy use of Sentinel CPS has shown a procedural success of greater than 90 %, achieving even 94-96% of successful implantation rate [1, 7]. Nevertheless, implantation failures have been reported in a few cases and are mostly associated with complex anatomical features such as vascular tortuosity, bovine aortic arch variants or arch steepness [7-9].

The majority of the trials investigating the application of the Sentinel-CPS during TAVI focus on its safety and feasibility features as well as on incidence of stroke rather than the reasons of CPD procedural failure. In fact, objective data about implantation failure of the Sentinel CPS device are still lacking. Therefore, we sought to investigate the reasons of Sentinel CPS device implantation failure, focusing on the anatomical features.

The failure of Sentinel CPS implantation was observed in 9.8% (n=9) of our patients undergoing filter-protected TAVR. This is in line with previous studies, demonstrating rates of unsuccessful device placements in 3.1% - 40% of patients [1, 5, 7, 8, 22]. Vascular tortuosity of the supra-aortic arteries was identified as the main reason for failure of Sentinel-CPS application in our cohort.

Arterial or vascular tortuosity is defined as the presence of abnormal twists and turns of one or several arteries [47]. Elongation and torquing of the vessels are mainly caused by structural changes of the vascular bed. A twisted vessel course requires an experienced catheter handling for wire advancement, to overcome acute and tortuous curves. Hence, extensive tortuosity of the supraaortic arteries could impede movement of the guidewire, and thus sufficient advancement of the Sentinel-CPS [23]. Moreover, repeated attempts to navigate and deploy the filter-based protection system in such unfavorable anatomical conditions might put the patient at a higher risk for perioperative complications [21]. As vessel tortuosity is associated with a higher arterial wall fragility, excessive catheter maneuvers might induce endothelial damage with vessel injury and dislodgment of debris ultimately causing cerebral emboli and ischemia [10, 15].

Case et colleagues published a post-market surveillance from the FDA MAUDE database in 2020 [12]. They reported on 4 cases of periprocedural stroke associated with Sentinel-CPS deployment difficulties due to vessel tortuosity.

Tortuous anatomy has been previously identified [7, 10, 11] but not quantified as a factor contributing to technical difficulty or device failure. The device-maker's instructions clearly stipulate that Sentinel-CPS insertion should be avoided in patients with 'excessive' vessel tortuosity. However, 'excessive' is not further defined [44]. With our present MSCT analysis we were finally able to solve this problem and for the first time numerically quantify "excessive" vessel tortuosity. Our measurements showed a brachiocephalic angle of 59°, a brachiocephalic TI of 26 and a right subclavian TI of 191 as threshold values beyond which failure of Sentinel-CPS application is likely to occur [44]. Of those, the brachiocephalic tortuosity angle could be detected as the most significant predicting factor with a sensitivity, specificity and AUC of 71.4%, 91.5% and 0.86 respectively.

This is the first study to demonstrate that difficulties of filter placement can be anticipated by anatomy assessment and highlight the importance of preoperative, standardized tortuosity calculation. Consequently, filter-based usage should be avoided in TAVR patients with a brachiocephalic angle >59° [44].

Further on, Sentinel CPS implantation failure is not only influenced by vascular morphology but also by anatomical characteristics of the aortic arch. The theory behind this concept is derived from previous studies of neuro-interventional procedures: Fagioli et al. in 2007 demonstrated that technical failure of the carotid artery stenting was independently associated with aortic arch anomaly (OR= 2.11, p = 0.005). Following this theory Tagliari et al. [9] investigated the feasibility and safety of implantation of the Sentinel-CPS in patients with abnormal aortic arch configurations,

specifically with bovine arch (n=145), vs patients with standard aortic arch anatomy (n = 20). Bovine arch anatomy is the most common variant in branching patterns of the aortic arch with a prevalence ranging from 8% to 30% in the general population. [9,50] It consists of a common origin of the brachiocephalic trunk and the left common carotid artery. Tagliari et al. demonstrated a significantly higher rate of Sentinel-CPS failure in patients with bovine anatomy compared to those with a normal aortic arch ($p = 0.002$) However, this was not reflected in an increased complication rate [9].

The main reason for technical failure in bovine arch anatomy might be due to its geometrical features, such as the severe angulation, steepness and elongation of the aortic arch and its supra-aortic vessels [9]. In case of bovine arch, the brachiocephalic trunk and the left common carotid artery share the same origin resulting in a more oblique vessel orientation of the left common carotid artery [51]. Sentinel-CPS implantation in those patients might fail due to more complex navigation of the Sentinel-CPS through the sharp turn between the aortic arch and the orifice of the left common carotid artery. [25]

In our cohort study bovine arch anatomy was found with an incidence of 20.6 % which is similar to the general literature. Nevertheless, there were no differences observed in the rate of device failure among our patients with and without bovine anomaly.

Apart from the branching pattern of the aortic arch, arch steepness, especially a Type III configuration, and sharp take-off angles of the supra-aortic branches were also identified as determinants for technical failure of Sentinel-CPS application in previous studies [15, 21, 26]. However, those were not associated with Sentinel-CPS failure in our patient cohort.

Our operators use an advanced technique to deploy the Sentinel CPS device, which consists of an extreme flexion of the distal part of the device using the integrated

articulation sheath that may help to advance the wire into the ostium of the left common carotid artery. This could be the reason why we did not find any associations between the aortic arch anatomical characteristics and Sentinel CPS implantation failure.

Vascular access site also plays an important role in the procedural insertion of the Sentinel CPS. In our cohort, extreme kinking of the right radial artery precluded successful Sentinel-CPS insertion in two patients. Access site related failure was also described by Seeger and colleagues in 2017 [22]. The study enrolled 802 consecutive patients undergoing TAVR, of whom 34.9% (n=280) received the Sentinel CPS. Both filters could be successfully positioned in 91.8% of patients. Device failure occurred in 59% of the patients due to heavily calcified or hypoplastic arteries at puncture sites.[22].

Device tracking can be difficult in case of tortuous radial artery, vasospasm or hypoplastic radial artery. In those situations, the tip of the guiding catheter can create a "razor blade effect" that prevents catheter navigation and sometimes even leads to perforation of the radial artery [8, 27]. Pigtail assisted tracking of the guiding catheter might help to overcome this effect, as it enables non-traumatic navigation of the guiding catheter through complex radial anatomy [27].

4.1.Limitations

This study reports the results of a retrospective and single-center investigation.

The ultimate population study is limited in size.

As this study focuses on MSCT-based identification of anatomical features potentially associated with Sentinel-CPS application failure, the correlation between failed device use and neurological outcome was not assessed.

In addition, technical factors in our study population might be confounded by advances in technique, operators experience and patient selection over the study period.

5. Summary and Conclusion

Despite significant advances in the field of structural heart disease, ischemic stroke continues to be a major complication associated with transcatheter aortic valve replacement (TAVR) [11,12]. To potentially reduce this risk, cerebral embolic protection device can be deployed to capture or deflect embolized material. The Sentinel CPS (Boston Scientific) is the first and so far only FDA-approved filter device to use during TAVR procedure to reduce the risk of stroke [17,23,24]. Multiple trials have shown Sentinel CPS strong safety profile and effective debris capture in 86%-99% of the patients [1, 3–5].

Given these data, the more widespread use of Sentinel-CPS in TAVI patients may be recommended.

In order to avoid periprocedural complications and potential device implantation failure, a pre-operative, standardized assessment of the vascular prerequisites for CPS insertion is imperative.

Objective data reported a Sentinel CPS successful implantation of 95-98% [1,7,71], and rates of unsuccessful device implantation range between 3,1% to 40% according to different studies [1, 5, 7, 8, 22]. In our cohort CPS device failure was observed in 9 patients (9.8%) due to the infeasibility to perform correct deployment of both filters (n = 7) and to obtain peripheral radial access (n = 2).

We further investigate on a multislice computed tomography pre-TAVR aortograms analysis the impact of aortic arch anatomy, configuration, and the angles of the supra-aortic arteries, including the determination of vascular tortuosity index on device failure of Sentinel-CPS application.

Vascular tortuosity of the right brachiocephalic artery was for the first time identified as a predictive anatomical factor for technical failure of Sentinel-CPS application in TAVR. Supra-aortic arteries angulation could impede the catheter steering and guidewire handling, and therefore the correct navigation and ultimately positioning of the Sentinel CPS device. Vascular tortuosity has been previously described as potential reason for implantation failure but not yet confirmed as a predictive factor. Our aortogram CT analysis is the only study in the literature that shows how in case of a brachiocephalic angulation of 59°, a brachiocephalic Tortuosity Index of 26 and a subclavian TI of 191 failure of the Sentinel CPS is likely to occur. These cut off values could now finally clarify and quantify the device-maker's instruction that stipulates to avoid Sentinel CPS implantation in 'excessive' vessel tortuosity.

Consequently, our recommendation states to avoid filter implantation in patients with brachiocephalic measurements above this threshold.

Vascular tortuosity is simple, rapid to assess and requires no additional imaging, as the pre-TAVR multislice computed tomography aortogram provides all necessary calculations. In addition, standardized failure-reporting policies may improve existing device technology and enhance patients' safety and outcomes.[44]

6.List of Figures

1. Figure 1, Fanning JP, et al. Characterization of neurological injury in transcatheter aortic valve implantation: how clear is the picture?

Figure 1.A: Embrella Embolic Deflector device (EED) (Edwards Lifesciences; Irvine, California, United States) [68].....6

2. Figure 2., Sentinel™ Cerebral Protection System

Distal filter (1), steerable catheter (100 cm) (2) und proximal filter (3). (b+c) two cone-shaped filter made of a radiopaque Nitinol coat biocompatible polyurethane (with 140-µm pores) with a maximum diameter of 10mm distal (b) and 15mm proximal (c) [47].....14

3. Figure 3: Filterlanding zone in the aimed vessel ,Voss.S. (2022) Neuroprotektion bei Transkatether-Aortenklappenimplantation (Habilitation, Technische Universität München)

Aortic arch identification, (B) Deployment of both filters in the aimed vessels (C) graphic representation of filters deployment15

4. Figure 4 from S.Voss et al, interactive cardiovascular and thoracic surgery, multislice computed tomography measurements using the automated 3mensio software. (A) Centre line across the lumen of the distal target [44].....20

5. Figure 5, multislice computed tomography measurements using the automated 3mensio software: (A) normal aortic arch, (B) bovine arch Type I, (C) bovine arch type II.....21

6.	Figure 6 from S.Voss et al, interactive cardiovascular and thoracic surgery, multislice computed tomography measurements using the automated 3mensio software, Aortic arch type [44].....	22
7.	Figure 7, from S.Voss et al, interactive cardiovascular and thoracic surgery, multislice computed tomography measurements using the automated 3mensio software: Measurements of the take-off angles [44].....	23
8.	Figure 8, multislice computed tomography measurements using the automated 3mensio software: Inner great vessel angle (BA/CCA)	24
9.	Figure 9, from S.Voss et al, interactive cardiovascular and thoracic surgery, multislice computed tomography measurements using the automated 3mensio software: (A) Tortuosity Angle, (B) Tortuosity Index of brachiocephalic trunk (C) Tortuosity Index of the tight subclavian artery [44].....	26
10.	Figure 10, from S.Voss et al, interactive cardiovascular and thoracic surgery: Receiver operating characteristic curve (ROC) analysis for the brachiocephalic tortuosity angle (A), the brachiocephalic tortuosity index (B), and the subclavian tortuosity index (C). ROC analysis was only performed in patients with Sentinel™ Cerebral Protection System failure due to vascular tortuosity (n = 7) [44].....	34

7.List of Tables

1.	Table 1 Patients characteristics.....	31
2.	Table 2 Procedural characteristics.....	32
3.	Table 3 Intraoperative reasons for Sentinel-CPS failure.....	33
4.	Table 4 Aortic Arch Anatomy and aortic arch configuration.....	36
5.	Table 5 Introbserver agreement for 3-dimensional multislice computed tomography measurements.....	37
6.	Table 6 Interobserver agreement for 3-dimensional multislice computed tomography measurements.....	38

8. References

- [1] Kapadia SR, Kodali S, Makkar R, Mehran R, Lazar RM, Zivadinov R, Dwyer MG, Jilaihawi H, Virmani R, Anwaruddin S, Thourani VH, Nazif T, Mangner N, Woitek F, Krishnaswamy A, Mick S, Chakravarty T, Nakamura M, McCabe JM, Satler L, Zajarias A, Szeto WY, Svensson L, Alu MC, White RM, Kraemer C, Parhizgar A, Leon MB, Linke A, Investigators ST. Protection Against Cerebral Embolism During Transcatheter Aortic Valve Replacement. *J Am Coll Cardiol* 2017;69:367-77.
- [2] Huded CP, Tuzcu EM, Krishnaswamy A, Mick SL, Kleiman NS, Svensson LG, Carroll J, Thourani VH, Kirtane AJ, Manandhar P, Kosinski AS, Vemulapalli S, Kapadia SR. Association Between Transcatheter Aortic Valve Replacement and Early Postprocedural Stroke. *Jama* 2019;321:2306-15.
- [3] Popma JJ, Deeb GM, Yakubov SJ, Mumtaz M, Gada H, O'Hair D, Bajwa T, Heiser JC, Merhi W, Kleiman NS, Askew J, Sorajja P, Rovin J, Chetcuti SJ, Adams DH, Teirstein PS, Zorn GL, 3rd, Forrest JK, Tchétché D, Resar J, Walton A, Piazza N, Ramlawi B, Robinson N, Petrossian G, Gleason TG, Oh JK, Boulware MJ, Qiao H, Mugglin AS, Reardon MJ. Transcatheter Aortic-Valve Replacement with a Self-Expanding Valve in Low-Risk Patients. *N Engl J Med* 2019;380:1706-15.
- [4] Van Mieghem NM, El Faquir N, Rahhab Z, Rodriguez-Olivares R, Wilschut J, Ouhlous M, Galema TW, Geleijnse ML, Kappetein AP, Schipper ME, de Jaegere PP. Incidence and predictors of debris embolizing to the brain during transcatheter aortic valve implantation. *JACC Cardiovasc Interv* 2015;8:718-24.
- [5] Van Mieghem NM, van Gils L, Ahmad H, van Kesteren F, van der Werf HW, Brueren G, Storm M, Lenzen M, Daemen J, van den Heuvel AF, Tonino P, Baan J, Koudstaal PJ, Schipper ME, van der Lugt A, de Jaegere PP. Filter-based cerebral embolic protection with transcatheter aortic valve implantation: the randomised MISTRAL-C trial. *EuroIntervention* 2016;12:499-507.
- [6] Schafer U. Safety and Efficacy of Protected Cardiac Intervention: Clinical Evidence for Sentinel Cerebral Embolic Protection. *Interv Cardiol* 2017;12:128-32.
- [7] Haussig S, Mangner N, Dwyer MG, Lehmkuhl L, Lucke C, Woitek F, Holzhey DM, Mohr FW, Gutberlet M, Zivadinov R, Schuler G, Linke A. Effect of a Cerebral Protection Device on Brain Lesions

Following Transcatheter Aortic Valve Implantation in Patients With Severe Aortic Stenosis: The CLEAN-TAVI Randomized Clinical Trial. *Jama* 2016;316:592-601.

[8] Naber CK, Ghanem A, Abizaid AA, Wolf A, Sinning JM, Werner N, Nickenig G, Schmitz T, Grube E. First-in-man use of a novel embolic protection device for patients undergoing transcatheter aortic valve implantation. *EuroIntervention* 2012;8:43-50.

[9] Tagliari AP, Ferrari E, Haager PK, Schmiady MO, Vicentini L, Gavazzoni M, Gennari M, Jorg L, Khattab AA, Blochlinger S, Maisano F, Taramasso M. Feasibility and Safety of Cerebral Embolic Protection Device Insertion in Bovine Aortic Arch Anatomy. *J Clin Med* 2020;9.

[10] Halkin A, Iyer SS, Roubin GS, Vitek J. Carotid artery stenting. In: Kipshidze NN, Fareed J, Moses JW, Serruys PW. *Textbook of Interventional Cardiovascular Pharmacology*. London, UK: Taylor & Francis Ltd.; 2007.p.555-69.

[11] Patel T, Shah S, Pancholy S, Deora S, Prajapati K, Coppola J, Gilchrist IC. Working through challenges of subclavian, innominate, and aortic arch regions during transradial approach. *Catheter Cardiovasc Interv* 2014;84:224-35.

[12] Case BC, Forrestal BJ, Yerasi C, Khan JM, Khalid N, Shlofmitz E, Chen Y, Musallam A, Chezar-Azerrad C, Satler LF, Ben-Dor I, Rogers T, Waksman R. Real-World Experience of the Sentinel Cerebral Protection Device: Insights From the FDA Manufacturer and User Facility Device Experience (MAUDE) Database. *Cardiovasc Revasc Med* 2020;21:235-38.

[13] Voss S, Deutsch MA, Schechtl J, Erlebach M, Sideris K, Lange R, Bleiziffer S. Impact of a Two-Filter Cerebral Embolic Protection Device on the Complexity and Risk of Transcatheter Aortic Valve Replacement. *Thorac Cardiovasc Surg* 2019.

[14] Voss S, Nobauer C, Lange R, Bleiziffer S. Cerebral protection during transcatheter aortic valve implantation in an extreme high-risk patient. *Eur J Cardiothorac Surg* 2017;52:998-99.

[15] Muller MD, Ahlhelm FJ, von Hessling A, Doig D, Nederkoorn PJ, Macdonald S, Lyrer PA, van der Lugt A, Hendrikse J, Stippich C, van der Worp HB, Richards T, Brown MM, Engelter ST, Bonati LH. Vascular Anatomy Predicts the Risk of Cerebral Ischemia in Patients Randomized to Carotid Stenting Versus Endarterectomy. *Stroke* 2017;48:1285-92.

- [16] Morris SA, Orbach DB, Geva T, Singh MN, Gauvreau K, Lacro RV. Increased vertebral artery tortuosity index is associated with adverse outcomes in children and young adults with connective tissue disorders. *Circulation* 2011;124:388-96.
- [17] Faggioli G, Ferri M, Gargiulo M, Freyrie A, Fratesi F, Manzoli L, Stella A. Measurement and impact of proximal and distal tortuosity in carotid stenting procedures. *J Vasc Surg* 2007;46:1119-24
- [18] Koo TK, Li MY. A Guideline of Selecting and Reporting Intraclass Correlation Coefficients for Reliability Research. *J Chiropr Med* 2016;15:155-63.
- [19] Fluss R, Faraggi D, Reiser B. Estimation of the Youden Index and its associated cutoff point. *Biom J* 2005;47:458-72.
- [20] Voss S, Schechtel J, Nobauer C, Bleiziffer S, Lange R. Patient eligibility for application of a two-filter cerebral embolic protection device during transcatheter aortic valve implantation: does one size fit all? *Interact Cardiovasc Thorac Surg* 2020.
- [21] Naggara O, Touze E, Beyssen B, Trinquart L, Chatellier G, Meder JF, Mas JL, Investigators E-S. Anatomical and technical factors associated with stroke or death during carotid angioplasty and stenting: results from the endarterectomy versus angioplasty in patients with symptomatic severe carotid stenosis (EVA-3S) trial and systematic review. *Stroke* 2011;42:380-8.
- [22] Seeger J, Gonska B, Otto M, Rottbauer W, Wohrle J. Cerebral Embolic Protection During Transcatheter Aortic Valve Replacement Significantly Reduces Death and Stroke Compared With Unprotected Procedures. *JACC Cardiovasc Interv* 2017;10:2297-303.
- [23] Rigatelli G, Dell'avvocata F, Vassiliev D, Daggubati R, Nanjiundappa A, Giordan M, Al Azza K, Cardaioli P, Nguyen T. Strategies to overcome hostile subclavian anatomy during transradial coronary angiography and interventions: impact on fluoroscopy, procedural time, complications, and radial patency. *J Interv Cardiol* 2014;27:428-34.
- [24] Faggioli GL, Ferri M, Freyrie A, Gargiulo M, Fratesi F, Rossi C, Manzoli L, Stella A. Aortic arch anomalies are associated with increased risk of neurological events in carotid stent procedures. *Eur J Vasc Endovasc Surg* 2007;33:436-41.
- [25] Ahn SS, Chen SW, Miller TJ, Chen JF. What is the true incidence of anomalous bovine left common carotid artery configuration? *Ann Vasc Surg* 2014;28:381-5.

- [26] Lam RC, Lin SC, DeRubertis B, Hyncek R, Kent KC, Faries PL. The impact of increasing age on anatomic factors affecting carotid angioplasty and stenting. *J Vasc Surg* 2007;45:875-80.
- [27] Garg N, Sahoo D, Goel PK. Pigtail assisted tracking of guide catheter for navigating the difficult radial: Overcoming the "razor effect". *Indian Heart J* 2016;68:355-60.
- [28] Coffey S, Cairns BJ, lung B. The modern epidemiology of heart valve disease. *Heart*. 2016;102:75-85.
- [29] Carapetis JR, Steer AC, Mulholland EK, Weber M. The global burden of group A streptococcal diseases. *Lancet Infect Dis*. 2005;5:685-94
- [30] Andras P. Durko1*, Ruben L. Osnabrugge1, Nicolas M. Van Mieghem2, Milan Milojevic1, Annual number of candidates for transcatheter aortic valve implantation per country: current estimates and future projections, *European Heart Journal* (2018) 39 2635–2642 doi:10.1093/eurheartj/ehy107
- [31] Costa G, Criscione E, Todaro D, Tamburino C, Barbanti M. Long-term Transcatheter Aortic Valve Durability. *Interv Cardiol*. 2019 May 21;14(2):62-69. doi: 10.15420/icr.2019.4.2. PMID: 31178931; PMCID: PMC6545973.
- [32] Eberhard Grube and Jan-Malte Sinning, The “Big Five” Complications After Transcatheter Aortic Valve Replacement: Do We Still Have to Be Afraid of Them? *J Am Coll Cardiol Intv*. 2019 Feb, 12 (4) 370–372
- [33] VARC-3 WRITING COMMITTEE, Généreux P, Piazza N, Alu MC, Nazif T, Hahn RT, Pibarot P, Bax JJ, Leipsic JA, Blanke P, Blackstone EH, Finn MT, Kapadia S, Linke A, Mack MJ, Makkar R, Mehran R, Popma JJ, Reardon M, Rodes-Cabau J, Van Mieghem NM, Webb JG, Cohen DJ, Leon MB. Valve Academic Research Consortium 3: updated endpoint definitions for aortic valve clinical research. *Eur Heart J*. 2021 May 14;42(19):1825-1857. doi: 10.1093/eurheartj/ehaa799. PMID: 33871579.
- [34] Pujari S., Agasthi P. *Aortic Stenosis StatPearls Publishing*; 2022 Jan.
- [35] C. Wand, Clinical significance of the bicuspid aortic valve content, *BMJ,Heart*, 2000
- [36] Figulla H.R. Franz M., Lauten A., *Cardiovasc Revasc Med*, The History of Transcatheter Aortic Valve Implantation (TAVI)-A Personal View Over 25 Years of development, *Cardiovasc Revasc Med*, Mar 2020, 398-403.

- [37] Barbanti M, Webb JG, Gilard M, et al. Transcatheter aortic valve implantation in 2017: state of the art. *EuroIntervention*. 2017;13:AA11-AA21.
- [38] Bjursten, H., Norrving, B. & Ragnarsson, S. Late stroke after transcatheter aortic valve replacement: a nationwide study. *Sci Rep* 11, 9593 (2021).
- [39] Huded, C. P. et al. Association between transcatheter aortic valve replacement and early postprocedural stroke. *JAMA* 321(23), 2306–2315 (2019)
- [40] Aggarwal SK, Delahunty Rn N, Menezes LJ, Perry R, Wong B, Reinthaler M et al. Patterns of solid particle embolization during transcatheter aortic valve implantation and correlation with aortic valve calcification. *J Interv Cardiol* 2018;31:648-54.
- [41] Haussig S, Linke A, Mangner N. Cerebral Protection Devices during Transcatheter Interventions: Indications, Benefits, and Limitations. *Curr Cardiol Rep*. 2020 Jul 10;22(9):96. doi: 10.1007/s11886-020-01335-9. PMID: 32651654; PMCID: PMC7351861.
- [42] N. M. Van Mieghem and J. Daemen, Reflections on the Fate of Cerebral Embolic Protection Devices With TAVR: The REFLECT II Trial, *JAm Coll Cardiol Intv*. 2021 Mar, 14 (5) 528–530
- [43] Schmidt T, Akdag O, Wohlmuth P, Thielsen T, Schewel D, Schewel J et al. Histological findings and predictors of cerebral debris from transcatheter aortic valve replacement: the ALSTER experience. *J Am Heart Assoc* 2016;5:e004399
- [44] S.Voss, C.Campanella, M.Burri, T. Trenkwalder, Anatomical reasons for technical failure of dual-filter cerebral embolic protection application in TAVR: a CT-based analysis, *J Card Surg*, 2021 Dec
- [45] Goldberg I, Auriel E, Russell D, Korczyn AD. Microembolism, silent brain infarcts and dementia. *Journal of the neurological sciences* 2012;322:250-3.
- [46] Kahlert P, Knipp SC, Schlamann M, Thielmann M, Al-Rashid F, Weber M et al. Silent and apparent cerebral ischemia after percutaneous transfemoral aortic valve implantation: a diffusion-weighted magnetic resonance imaging study. *Circulation* 2010;121:870-8.
- [47] Voss S, Lange R. Filterbasierte Neuroprotektion bei Transkatheter-Aortenklappenimplantation. *Zeitschrift für Herz-,Thorax- und Gefäßchirurgie* 2020;34:137-42

- [50] Layton, K.F.; Kallmes, D.F.; Cloft, H.J.; Lindell, E.P.; Cox, V.S. Bovine aortic arch variant in humans: Clarification of a common misnomer. *AJNR Am. J. Neuroradiol.* 2006, 27, 1541–1542.
- [51] N. Elsaid, G. Bigliardi, M.L. Dell'acqua, et al. The Relation Between Aortic Arch Branching Types and the Laterality of Cardio-Embolic Stroke, *J Stroke Cerebrovasc Dis*, 2020 Jul;29(7):104917
- [52] Camm, A. John and others (eds), *The ESC Textbook of Cardiovascular Medicine*, 3 edn, The European Society of Cardiology Series (Oxford, 2018; online edn, ESC Publications, 1 July 2018),
- [53] Rheude T, Pellegrini C, Lessmann L, Wiebe J, Mayr NP, Michel J, Trenkwalder T, Kasel AM, Schunkert H, Kastrati A, Joner M, Husser O, Hengstenberg C. Prevalence and Clinical Impact of Iron Deficiency in Patients With Severe Aortic Stenosis Referred for Transcatheter Aortic Valve Implantation. *Am J Cardiol.* 2019 Aug 7. pii: S0002-9149(19)30882-3.
- [54] Pellegrini C, Rheude T, Mahr L, Trenkwalder T, Mayr NP, Michel J, Schunkert H, Kasel AM, Joner M, Hengstenberg C, Kastrati A, Husser O, Kessler T. Influence of marital status in patients undergoing transcatheter aortic valve implantation. *J Thorac Dis.* 2019 May;11(5):1888-1895.
- [55] Trenkwalder T, Schunkert H, Reinhard W. [Cardiac involvement in storage diseases : Role of genetic diagnostics]. *Herz.* 2019 Aug;44(5):461-474.
- [56] Grabert S, Lange R, Bleiziffer S. Incidence and causes of silent and symptomatic stroke following surgical and transcatheter aortic valve replacement: a comprehensive review. *Interact Cardiovasc Thorac Surg.* 2016 Sep;23(3):469-76. doi: 10.1093/icvts/ivw142. Epub 2016 May 30. PMID: 27241049.
- [57] Leon MB, Smith CR, Mack M, et al; PARTNER Trial Investigators. Transcatheter aortic-valve implantation for aortic stenosis in patients who cannot undergo surgery. *N Engl J Med.* 2010;363:1597–1607.
- [58] Hatoum H, Samaee M, Sathananthan J, Sellers S, Kuetting M, Lilly SM, Ihdahid AR, Blanke P, Leipsic J, Thourani VH, Dasi LP. Comparison of performance of self-expanding and balloon-expandable transcatheter aortic valves. *JTCVS Open.* 2022 Apr 20;10:128-139. doi: 10.1016/j.xjon.2022.04.015. PMID: 36004225; PMCID: PMC9390782.
- [59] Gabor Erdoes, Reto Basciani, Christoph Huber, Stefan Stortecky, Peter Wenaweser, Stephan Windecker, Thierry Carrel, Balthasar Eberle, Transcranial Doppler-detected cerebral embolic load

during transcatheter aortic valve implantation, *European Journal of Cardio-Thoracic Surgery*, Volume 41, Issue 4, April 2012, Pages 778–784

[60] Kapadia SR, Huded CP, Kodali SK, Svensson LG, Tuzcu EM, Baron SJ, Cohen DJ, Miller DC, Thourani VH, Herrmann HC, Mack MJ, Szerlip M, Makkar RR, Webb JG, Smith CR, Rajeswaran J, Blackstone EH, Leon MB; PARTNER Trial Investigators. Stroke After Surgical Versus Transfemoral Transcatheter Aortic Valve Replacement in the PARTNER Trial. *J Am Coll Cardiol*. 2018 Nov 13;72(20):2415-2426. doi: 10.1016/j.jacc.2018.08.2172. PMID: 30442284.

[61] Eschenbach LK, Erlebach M, Deutsch MA, Ruge H, Bleiziffer S, Holzer L, Krane M, Voss S, Lange R, Burri M. Stroke after transcatheter aortic valve replacement: A severe complication with low predictability. *Catheter Cardiovasc Interv*. 2022 May;99(6):1897-1905. doi: 10.1002/ccd.30143. Epub 2022 Mar 21. PMID: 35312220.

[62] Armijo G, Nombela-Franco L, Tirado-Conte G. Cerebrovascular Events After Transcatheter Aortic Valve Implantation. *Front Cardiovasc Med*. 2018 Jul 31;5:104. doi: 10.3389/fcvm.2018.00104. PMID: 30109235; PMCID: PMC6080138.

[63] Woldendorp K, Indja B, Bannon PG, Fanning JP, Plunkett BT, Grieve SM. Silent brain infarcts and early cognitive outcomes after transcatheter aortic valve implantation: a systematic review and meta-analysis. *Eur Heart J*. 2021 Mar 7;42(10):1004-1015. doi: 10.1093/eurheartj/ehab002. PMID: 33517376.

[64] Demir OM, Iannopollo G, Mangieri A, Ancona MB, Regazzoli D, Mitomo S, Colombo A, Weisz G, Latib A. The Role of Cerebral Embolic Protection Devices During Transcatheter Aortic Valve Replacement. *Front Cardiovasc Med*. 2018 Oct 23;5:150. doi: 10.3389/fcvm.2018.00150. PMID: 30406115; PMCID: PMC6205957.

[65] Lansky AJ, Schofer J, Tchetché D, Stella P, Pietras CG, Parise H, Abrams K, Forrest JK, Cleman M, Reinöhl J, Cuisset T, Blackman D, Bolotin G, Spitzer S, Kappert U, Gilard M, Modine T, Hildick-Smith D, Haude M, Margolis P, Brickman AM, Voros S, Baumbach A. A prospective randomized evaluation of the TriGuard™ HDH embolic DEFLECTION device during transcatheter aortic valve implantation: results from the DEFLECT III trial. *Eur Heart J*. 2015 Aug 14;36(31):2070-2078. doi: 10.1093/eurheartj/ehv191. Epub 2015 May 19. PMID: 25990342.

- [66] Hajian-Tilaki K. Receiver Operating Characteristic (ROC) Curve Analysis for Medical Diagnostic Test Evaluation. *Caspian J Intern Med.* 2013 Spring;4(2):627-35. PMID: 24009950; PMCID: PMC3755824.
- [67] Rodés-Cabau J, Kahlert P, Neumann FJ, Schymik G, Webb JG, Amarenco P, et al.. Feasibility and exploratory efficacy evaluation of the Embrella Embolic Deflector system for the prevention of cerebral emboli in patients undergoing transcatheter aortic valve replacement: the PROTAVI-C pilot study. *JACC Cardiovasc Interv.* (2014) 7:1146–55. 10.1016/j.jcin.2014.04.019
- [68] Fanning JP, Walters DL, Platts DG, Eeles E, Bellapart J, Fraser JF. Characterization of neurological injury in transcatheter aortic valve implantation: how clear is the picture? *Circulation.* 2014 Jan 28;129(4):504-15. doi: 10.1161/CIRCULATIONAHA.113.004103. PMID: 24470472.
- [69] Baumbach A, Mullen M, Brickman AM, Aggarwal SK, Pietras CG, Forrest JK, Hildick-Smith D, Meller SM, Gambone L, den Heijer P, Margolis P, Voros S, Lansky AJ. Safety and performance of a novel embolic deflection device in patients undergoing transcatheter aortic valve replacement: results from the DEFLECT I study. *EuroIntervention.* 2015 May;11(1):75-84. doi: 10.4244/EIJY15M04_01. PMID: 25868876.
- [70] Nazif TM, Moses J, Sharma R, Dhoble A, Rovin J, Brown D, Horwitz P, Makkar R, Stoler R, Forrest J, Messé S, Dickerman S, Brennan J, Zivadinov R, Dwyer MG, Lansky AJ; REFLECT II Trial Investigators. Randomized Evaluation of TriGuard 3 Cerebral Embolic Protection After Transcatheter Aortic Valve Replacement: REFLECT II. *JACC Cardiovasc Interv.* 2021 Mar 8;14(5):515-527. doi: 10.1016/j.jcin.2020.11.011. Epub 2021 Mar 1. PMID: 33663779.
- [71] Van Mieghem NM, van Gils L, Ahmad H, van Kesteren F, van der Werf HW, Brueren G, Storm M, Lenzen M, Daemen J, van den Heuvel AF, Tonino P, Baan J, Koudstaal PJ, Schipper ME, van der Lugt A, de Jaegere PP. Filter-based cerebral embolic protection with transcatheter aortic valve implantation: the randomised MISTRAL-C trial. *EuroIntervention.* 2016 Jul 20;12(4):499-507. doi: 10.4244/EIJV12I4A84. PMID: 27436602.
- [72] Kapadia SR, Makkar R, Leon M, Abdel-Wahab M, Waggoner T, Massberg S, Rottbauer W, Horr S, Sondergaard L, Karha J, Gooley R, Satler L, Stoler RC, Messé SR, Baron SJ, Seeger J, Kodali S, Krishnaswamy A, Thourani VH, Harrington K, Pocock S, Modolo R, Allocco DJ, Meredith IT, Linke A; PROTECTED TAVR Investigators. Cerebral Embolic Protection during Transcatheter Aortic-Valve

Replacement. N Engl J Med. 2022 Oct 6;387(14):1253-1263. doi: 10.1056/NEJMoa2204961. Epub 2022 Sep 17. PMID: 36121045.

[73] Carroll JD, Saver JL. Does Capturing Debris during TAVR Prevent Strokes? N Engl J Med. 2022 Oct 6;387(14):1318-1319. doi: 10.1056/NEJMe2210185. Epub 2022 Sep 17. PMID: 36121036.

Acknowledgements

I would like to thank Prof. PD. Dr. Rüdiger Lange for the opportunity to work on this exciting project and PD. Dr. Keti Vitanova, my supervisor, for her support of this dissertation over the years.

My special thanks go to PD. Dr. med. Stephanie Voss for her great patience and encouragement during my doctorate. She spent a lot of energy and time mentoring me, giving me the professional advice that has broaden my sight. Through our inspiring discussions, I could learn a lot and grow not only in an academic way but also as person.

I would also like to express my sincere appreciation to PD. Dr. med. Theresa Trenkwalder, for her great support.

To my colleague and friend Miriam Lang for the many years of reliable cooperation and our precious friendship.

A big thank you goes to my colleagues at the German Heart Center in Munich.

Finally, a special thanks goes to my family, to whom I own the greatest debt of gratitude for always being at my side, with unconditional love and support. To my mom and Massimo, without you I could have never become the person and doctor that I'm today.

Dissertation based paper

(pdf)